Advanced Steel Construction – Vol. 20 No. 3 (2024) 292–299
DOI:10.18057/IJASC.2024.20.3.8

BENDING ANALYSIS OF RECYCLED CONCRETE BEAMS REINFORCED WITH GFRP BARS UNDER HIGH TEMPERATURE

Qi Guo [1, 2] and Hao Chen [3, *]

[1] *School of Civil Engineering, Xi'an University of Architecture and Technology, Xi'an 710055, Shanxi, China.*
[2] *Key Lab of Structural Engineering and Earthquake Resistance, Ministry of Education (XAUAT), Xi'an 710055, Shanxi, China.*
[3] *XAUAT UniSA An De College, Xi'an University of Architecture and Technology, Xi'an 710311, Shanxi, China*
** (Corresponding author: E-mail: 1054686243@qq.com)*

ABSTRACT

GFRP (Fiber Reinforced Polymer) reinforcement material is characterized by high strength and excellent corrosion resistance, which exhibits promising application prospects in engineering. The GFRP reinforcement for steel-concrete beams can increase the structural load-bearing capacity and durability. In this study, a refined finite element model of high-temperature GFRP-reinforced recycled steel-concrete beams was established by using ABAQUS software. The temperature distribution and residual load-carrying capacity of GFRP-reinforced recycled steel-concrete beams were analyzed, and the reliability of the model was validated based on the results of full-scale experiments on 16 groups of recycled steel-concrete beams. By using the validated model, the influence of heating temperature, reinforcement strength, steel strength, strengthening method, and concrete strength on the residual load-carrying capacity of the structure was analyzed. The stress patterns and failure mechanisms of GFRP-reinforced recycled steel-concrete beams were also analyzed. As can be seen from the results, the Type II strengthening method significantly increased the load-carrying capacity of recycled steel-concrete beams. It was also found that the load-carrying capacity of the tested beams was greatly affected by temperature. Under the temperature of 200℃ and 600℃, the load-carrying capacity of the unreinforced specimens decreases by approximately 13% and around 25%, respectively. Under the same heating temperature, compared to the unreinforced specimens, the load-carrying capacity was increased by approximately 10% by using the Type I strengthening method, but only around 4.7% by the Type II strengthening method. Finally, based on the results of this study and existing relevant experimental and numerical simulation results, and considering its feasibility and effectiveness, the Type I strengthening method for reinforced recycled steel-concrete beams was proposed. In general, the research findings of this paper can provide theoretical support for the design of reinforced recycled steel-concrete beams.

ARTICLE HISTORY

Received: 13 November 2023
Revised: 28 May 2024
Accepted: 11 June 2024

KEYWORDS

GFRP reinforcement;
High temperature;
Steel-reinforced recycled aggregate concrete beams;
Residual load-carrying capacity;
Bending performance

1. Introduction

Green and energy conservation are increasingly prevailing in the development of the construction industry. The application of new materials and new structures can better protect the environment [1-2], and Glass Fiber Reinforced Plastic Fiber (GFRP) is such a new type of green high-performance material with prominent advantages of lightweight, high strength, great corrosion resistance, and easy machinability, which has been widely used in practical engineering structures [3-5]. Research shows that the compressive strength and elastic modulus of recycled aggregate concrete (RCAC) are lower than that of ordinary concrete, while its strength and durability can be improved by changing the addition method of admixtures. [6-10] Compared to ordinary reinforced concrete beams, steel-reinforced recycled aggregate concrete (SRRAC) [11-14] is advantageous in load-carrying capacity and stiffness, which is mainly due to the mutual restraint and effective force collaboration between steel and concrete. Moreover, as an environmentally friendly material, recycled concrete can address the pollution caused by construction waste. The GFRP reinforcement for recycled steel-concrete beams enhances, on the other hand, the load-carrying capacity and durability of the structure. However, the high-temperature caused by fires can deteriorate the GFRP reinforcement, consequently impacting the overall durability, load-carrying capacity, and even threatening the structural safety.

Currently, scholars from China and abroad have conducted systematic studies on the mechanical properties of recycled concrete beams reinforced with steel at both room temperature and above, including experimental research, numerical simulations, and theoretical analysis. [15-20] Chen et al. proposed a new structure of steel-reinforced recycled aggregate concrete (SRRAC), thereby using the confinement effect of section steel sections to compensate for the deficiencies of RA [21]. Danying Gao, et al. conducted a four-point bending test on 13 beams, and found that the shear bearing capacity of recycled aggregate and steel fiber concrete beams decreased with the increase of the replacement rate of recycled coarse aggregate. In the meantime, the volume of steel fiber gradually increases as the score increases. Emmanuel E. Anike et al. [22] found that the bearing capacity of hybrid beams prepared by conventional methods, containing 100% recycled aggregate (RA) and 1% steel fiber (SF) is comparable to that of similar mixtures without SF and the reference. Compared with the mixture, it has increased by 13% and 8%, respectively. Arash Karimi Pour et al. [23] studied the influence of simultaneous effects of GFRP and PP fibers on improving the shear properties of high-strength (HS) recycled coarse aggregate (RCA) concrete beams. The test was conducted on 36 RC beams fabricated, showing that as the RCA content increased, PP fibers were more effective in enhancing the shear properties of GFRP steel-reinforced high-strength concrete (HSC) beams. Faraz Tariq et al. [24] studied the mechanical properties and bonding properties of fire-exposed recycled coarse and fine aggregate concrete (RAC), and provided the load and residual slip as well as bond temperature relationships and subsequent deterioration based on the test result. A model of interrelationships was proposed to help in the prediction of the performance of structural elements made of RAC after exposure to fire or high temperature. Zongping Chen et al. [25] studied the eccentric compression behavior of recycled aggregate concrete (RRAC) columns at high temperature by means of experiments and numerical simulations. They found that temperature is the main factor affecting the eccentric compression behavior, followed by eccentricity, and the replacement percentage of RCA. They also proposed an equivalent model for the residual bearing capacity of RRAC columns. Xue Jianyang et al. [26] conducted comparative experimental research on ordinary steel-reinforced concrete beams and steel-reinforced recycled concrete beams, with concrete strength, shear-span ratio, and replacement of recycled aggregate as experimental parameters. As can be seen from the study, the two types of beams exhibited similar load-carrying mechanisms, and the strength reduction of the steel-reinforced recycled concrete beams was not significant compared to ordinary steel-reinforced concrete beams. Wu Ping Chuan et al. [27] conducted static load tests on four groups of steel recycled concrete beams, and observed the failure modes of the test beams. In the study, the aggregate replacement rate was found to have little impact on the bearing capacity of the test beams. Chen Zongping et al. [28] conducted comparative experimental research on steel-reinforced concrete specimens, focusing on the replacement rate of recycled coarse aggregate, bonding location between steel and recycled concrete, and the thickness of the steel protection layer. In the study, they proposed a calculation and prediction formula for the bonding strength between steel and concrete. Han Fei et al. [29] carried out flexural performance tests on basalt fiber-reinforced polymer (BFRP) reinforced recycled concrete beams and ordinary reinforced recycled concrete beams. It was revealed that BFRP-reinforced recycled concrete beams exhibited superior ductility and load-carrying capacity compared to ordinary reinforced recycled concrete beams. In the experimental research on steel-reinforced recycled concrete beams after exposure to high temperatures, Chen Zongping et al. considered the heating temperature and replacement rate of recycled aggregate as experimental parameters, and revealed the bending failure and damage mechanism of steel-reinforced recycled concrete

beams after high-temperature exposure. Additionally, they proposed a calculation formula for predicting the residual load-carrying capacity of steel-reinforced recycled concrete beams after high-temperature exposure. Furthermore, scholars from China and abroad conducted experimental studies and analysis on the mechanical performance degradation of FRP reinforcement after exposure to high temperatures with substantial research achievements in this field. For instance, Lu Chunhua et al. [31] conducted experimental research on the tensile properties of two types of FRP reinforcements (BFRP and GFRP), and observed the microstructure of the two types of reinforcements after high-temperature damage using scanning electron microscopy. Based on the experimental results, they proposed a tensile strength degradation model for both types of reinforcements in the temperature range of 20-220°C. Gao Yong Hong et al. [32] analyzed the tensile strength characteristics of GFRP reinforcement with different steel bar diameters (16mm, 22mm and 25mm) after exposure to high temperatures, using the steel bar diameter as an experimental parameter. Based on the relationships established between the ultimate tensile strength, ultimate elongation, elastic modulus, and temperature, extensive research has been conducted on the mechanical properties of steel-reinforced recycled concrete beams under ambient and high-temperature conditions, as well as on the degradation of FRP reinforcement after high-temperature exposure. However, the research on high-temperature GFRP-reinforced recycled concrete beams is limited. To explore the influence of GFRP reinforcement strength and strengthening methods on the load-carrying capacity of steel-reinforced recycled concrete beams, a refined finite element model of high-temperature GFRP-reinforced steel-recycled concrete beams was established by using ABAQUS software. The accuracy and reliability of the model were validated by the full-scale experimental results of high-temperature steel-reinforced recycled concrete beams from both domestic and international sources. Furthermore, parameter analysis was performed to find out the factors influencing the high-temperature steel-reinforced recycled concrete beams. The accuracy of the composite beam design method as specified in GB 50017-2017 [33] “Code for Design of Steel Structures" was evaluated based on the finite element analysis results and using the variability analysis approach. Consequently, a design method considering GFRP reinforcement for steel-reinforced recycled concrete beams was proposed.

2. Establishment of finite element model

2.1. Overview of the model

Finite element model of GFRP-reinforced recycled concrete beams for vertical shear performance was established by using ABAQUS software. The model mainly includes I-shaped steel beams, GFRP reinforcement bars, steel bars, and concrete beams, etc. The 3D structure of the recycled concrete beams with I-shaped steel is shown in Fig. 1(a), and the established finite element model is shown in Fig. 1(b).

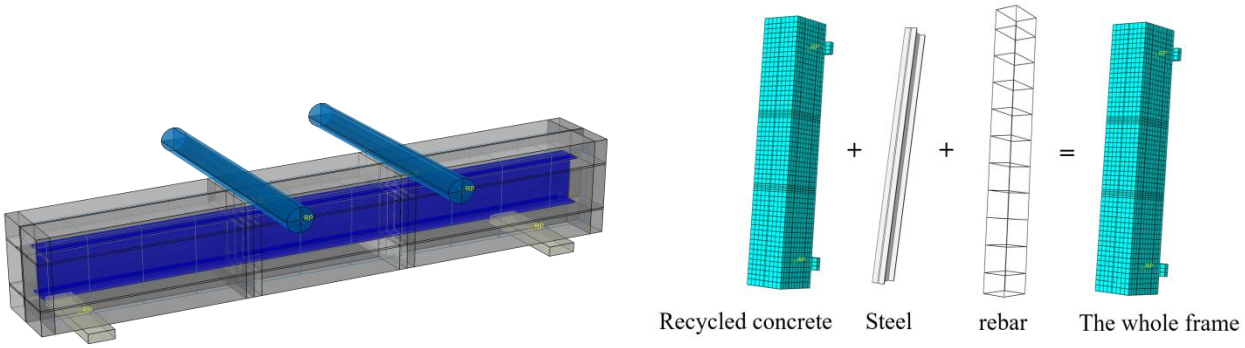

(a) 3D structure diagram (b) Finite element analysis model of component

Fig. 1 Schematic diagram of steel reinforced recycled concrete beam

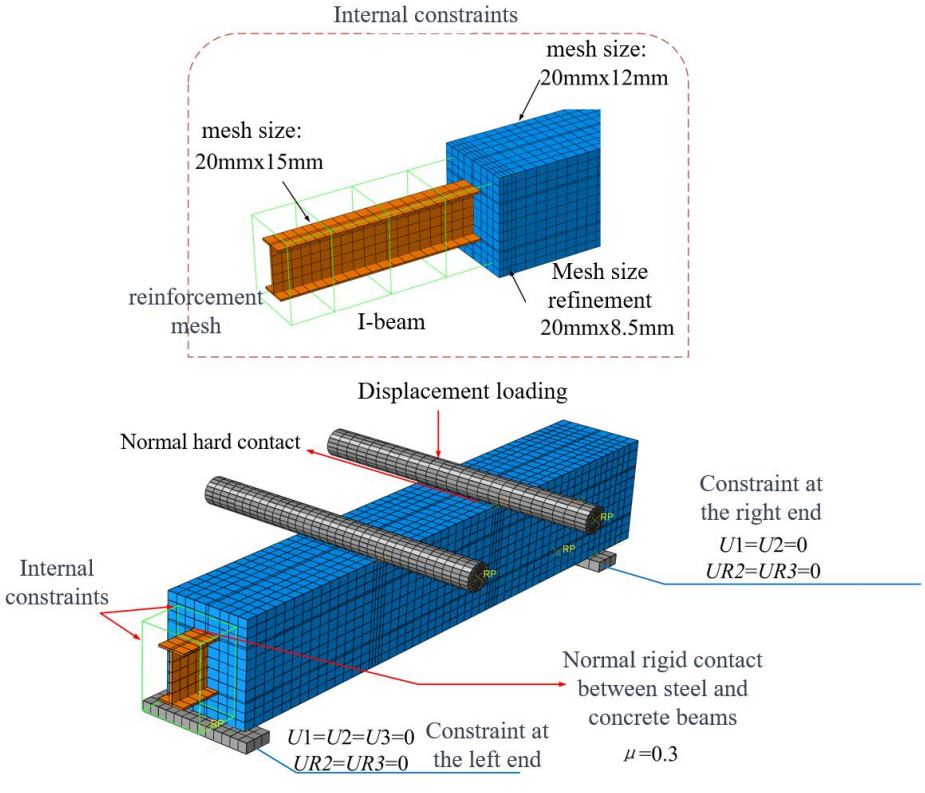

Fig. 2 Interaction and Boundary Condition Setting of GFRP Reinforcement Reinforced Steel Recycled Concrete Beams

2.2. Element selection and mesh division

The model of GFRP-reinforced recycled concrete beams was established based on three types of elements, namely, I-shaped steel beams, bearing pads, and concrete beams, using hexahedral eight-node solid elements (C3D8R). On the other hand, the longitudinal bars and stirrups were simulated using truss elements (T3D2). To improve the computational accuracy, during mesh division, the mesh element size of the concrete beams is set to be up to 15mm, ensuring a minimum of 4 elements in the thickness direction to satisfy the requirements of integral calculations, and avoid numerical singularities. The element size of the steel beams is controlled within 20mm, and that of the steel bars does not exceed 20mm. A "void" operation is performed in the concrete beams to accommodate the placement of I-shaped steel beams, which enables the interaction of bond-slip between the steel beams and the concrete beams.

To ensure the smooth introduction of the temperature field ODB file, the mesh partitioning of the temperature field model and the mechanical model of GFRP-reinforced recycled concrete beams must be identical.

2.3. Interaction and boundary condition settings

The interaction settings for the components of the GFRP-reinforced recycled concrete beam model are as follows.

(1) The coupling of degrees of freedom between the steel reinforcement cage and the concrete beam is achieved through the built-in area command, which enables them to work together.

(2) Interactions are set at the interface between the steel beam and the concrete beam to define the bond-slip behavior between them.

(3) Thermal convection and thermal radiation are applied to the surface of the concrete to simulate heat conduction. The thermal convection coefficient is set to 25 W/(m^2·K), and the thermal radiation coefficient is set to 0.5. The I-shaped steel beam and the concrete are tied together during the temperature field analysis to enable heat transfer.

(4) The steel bars are bonded to the surface region of the concrete beam, and loading is achieved through the coupling of degrees of freedom.

(5) Binding constraints are applied between the steel beam and the loading pad.

The boundary conditions of the GFRP-reinforced recycled concrete beam test specimen are consistent with that of the experiment, with one end fixed and the other end hinged. Displacement-controlled loading is applied during the modeling, and the specific boundary and interaction settings are shown in Fig. 2.

2.4. Material constitutive models

The constitutive models of concrete and steel materials have to be determined in the finite element model. The specific constitutive models are as follows.

(1) Constitutive model of concrete: the concrete is modeled by using the concrete plastic damage (CDP) model, with a Poisson's ratio of 0.2[34]. The elastic modulus of ordinary concrete is calculated by using the equation specified in the European Concrete Design Code EC2-2004[33] as follows.

$$E_c = 22 \cdot (f_{cr}/10)^{0.3} \quad (1)$$

where f_{cr} represents the axial compressive strength of the concrete.

The $E_{C,RAC}$ model is adopted for recycled concrete, which considers the replacement ratio (k) and the residual mortar content Y_{RM} of recycled coarse aggregates, as described in Reference [35].

$$E_{C,RAC}=\left(1-{}^{2}/_{3}\cdot kY_{Rm}\right)E_C \quad (2)$$

where Y_{Rm} represents the residual mortar content, which is typically between 30% and 50% [36]. In the case of unknown residual mortar content, an average value of 40% can be used. k refers to the replacement ratio of recycled coarse aggregates.

The compressive stress-strain behavior of recycled concrete and ordinary concrete is simulated by using the concrete stress-strain model proposed by Xiao et al. [37], which accounts for the influence of the replacement ratio of recycled coarse aggregates, as illustrated in Fig. 4.The equation of the model is as follows：

$$\sigma_x = \begin{cases} m\varepsilon_x + (3-2m){\varepsilon_x}^2 + (m-2){\varepsilon_x}^2 & (0 \le \varepsilon_x < 1) \\ \dfrac{\varepsilon_x}{n(\varepsilon_x-1)^2+\varepsilon_x} & (\varepsilon_x \ge 1) \end{cases} \quad (3)$$

where ε_x represents the relative compressive strain of concrete, $\varepsilon_x = \varepsilon_c/\varepsilon_u$, ε_c refers to the compressive strain of concrete, ε_u stands for the peak compressive strain of concrete; σ_x denotes the relative compressive strength of concrete, $\sigma_x = \sigma_c/f_{cr}$， σ_c is the compressive stress of concrete, f_{cr}represents the axial compressive strength of concrete; and m and n are the influence factors of the replacement ratio of recycled coarse aggregates, which can be calculated by using the following equation.

$$m=2.2(0.478k^2 - 1.231k + 0.975)$$

$$n=0.8(7.664k + 1.142) \quad (4)$$

The tensile stress-strain relationship of recycled concrete is similar to that of ordinary concrete [38], and the concrete tensile stress-strain model proposed by Xiao et al. [37] is adopted, which is expressed as follows:

$$\sigma_{t,x} = p\varepsilon_{t,x} - (p-1)\varepsilon_{t,x}^6 \quad (5)$$

where $\varepsilon_{t,x}$represents the relative tensile strain of concrete, $\varepsilon_{t,x} = \varepsilon_t - \varepsilon_{tu}$, ε_t refers to the tensile strain of concrete, ε_{tu} denotes the peak tensile strain of concrete; $\varepsilon_{t,x}$ stands for the relative tensile strength of concrete, $\sigma_{t,x} = \sigma_t/f_{tu}$, σ_t is the tensile strength of concrete; and p refers to the ratio of tangent modulus to secant modulus at the reference point, which can be calculated by using the following equation:

$$P = 0.007k + 1.190 \quad (6)$$

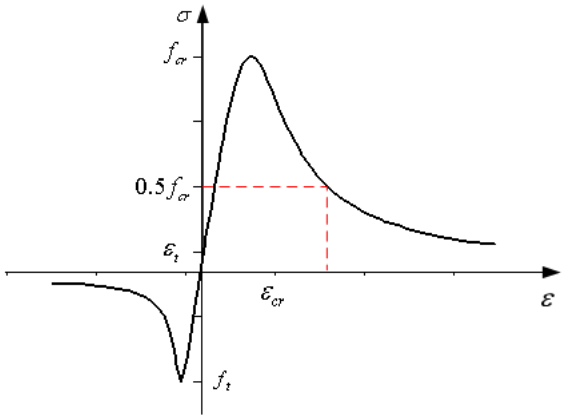

Fig. 3 Stress-strain curve of concrete

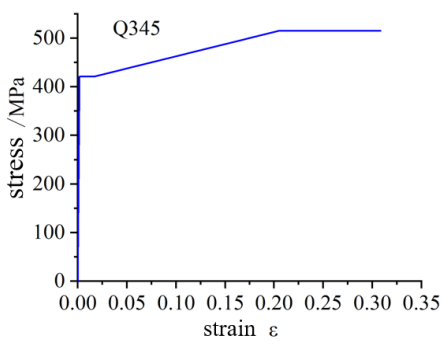

(a) Constitutive Model of Q345 and Bolts

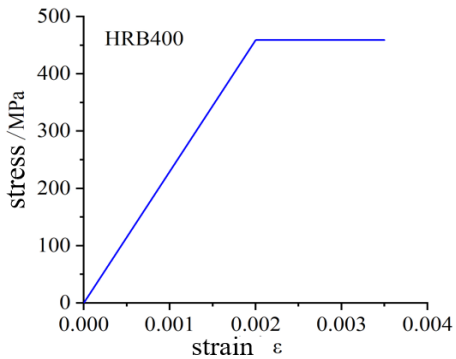

(b) Constitutive Model of HRB400 Reinforcing Steel

Fig. 4 Steel constitutive

2.5. Material constitutive model

The constitutive relationships for steel beams and bolts are shown in Fig. 4(a). The constitutive model for steel beams considers strain hardening at both room temperature and high temperature, while the steel reinforcement is calculated by using an ideal elastic-plastic model with the strength values determined based on the experimental results. The constitutive relationships are illustrated in Fig. 4(b).

$$\sigma = \begin{cases} E_s\varepsilon & \varepsilon \le \varepsilon_y \\ f_y & \varepsilon_y \le \varepsilon \end{cases} \quad (8)$$

where f_y represents the yield strength of the steel material; E_s refers to the elastic modulus of the steel material; and ε_y stands for the yield strain of the steel material.

2.6. Model verification

Finite element analysis was conducted on high-temperature recycled steel-reinforced concrete beams, as shown in [39], and the accuracy and feasibility of the model were verified by comparing the finite element simulation data with the experimental data obtained from previous studies.

2.6.1. Existing experimental parameters and results

Existing test results of steel-reinforced concrete composite beams using recycled materials were collected to validate the accuracy and feasibility of the finite element analysis. The parameters of the steel-reinforced concrete composite beam specimens employed in this study were as follows: length of 1100mm, width of 150mm, height of 200mm, protective layer thickness of 25mm, recycled concrete strength grade of C40, Steel type 10, Q345 for internal steel, longitudinal reinforcement of 14mm-diameter HRB335, stirrups of 6.5mm-diameter HPB300, temperatures of room temperature, 200°C, 400°C, and 600°C. Besides, the replacement rates were 0%, 30%, 70%, and 100%. The detailed cross-section of the test beam is shown in Fig. 5, and Table 1 summarizes the test parameters and results for all specimens.

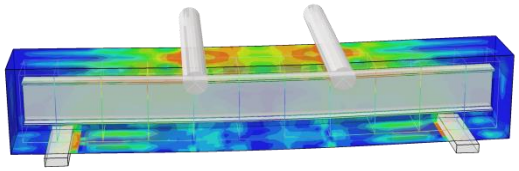

(a) Three-dimensional view of composite beam

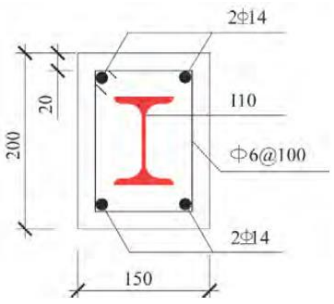

(b) Cross-section view at mid-span

Fig. 5 Detailed drawings of the test piece

2.6.2. Finite element model verification

Experimental research was conducted on steel-concrete beams using recycled concrete under room-temperature and high-temperature conditions, as shown in the reference [39]. Fig. 6 shows the comparison between the experimental and finite element results of the load-deflection curves of selected test beams. The error of simulated ultimate load values of the model created in ABAQUS ranges from 0.15% to 3.82% compared to the experimental values. It can be seen from the diagram that the overall distribution of the two curves is similar, and can be divided into three stages. The load-deflection curve of the steel-concrete beams using recycled concrete, obtained based on the thermal-structural coupling analysis method, is generally like the experimental curve with some differences. Overall, the difference between the two curves is within 10%, indicating a good agreement between the experimental results and the simulated values. The above results indicate that the finite element model can well predict the flexural performance of steel-concrete beams using recycled concrete. On this basis, further mechanical performance analysis can be conducted for GFRP-reinforced steel-concrete beams using recycled concrete.

Table 1
Major experimental parameters and results of steel-reinforced recycled composite beams

Test specimen number	K_0/kN·mm^{-1}	P_u/kN	θ	f_u/mm	Strength grade/MPa	T/℃	λ/%
SA-T25-0-1	153.8	249.5	2.0	4.06	C30	Room temperature	0
SA-T25-30-2	166.7	257.2	2.0	5.75	C30		30
SA-T25-70-3	200.0	255.3	2.0	7.11	C30		70
SA-T25-100-4	160.0	256.7	2.0	2.99	C30		100
SA-T200-0-1	103.4	255.4	2.0	3.39	C30	200	0
SA-T200-30-2	146.3	230.0	2.0	4.76	C30		30
SA-T200-70-3	171.4	237.9	2.0	5.15	C30		70
SA-T200-100-4	181.8	263.0	2.0	4.80	C30		100
SA-T400-0-1	136.4	234.0	2.0	4.37	C30	400	0
SA-T400-30-2	157.9	227.6	2.0	3.50	C30		30
SA-T400-70-3	126.6	242.7	2.0	5.64	C30		70
SA-T400-100-4	133.3	248.0	2.0	4.90	C30		100
SA-T600-0-1	92.0	188.4	2.0	4.67	C30	600	0
SA-T600-30-2	87.0	194.5	2.0	5.85	C30		30
SA-T600-70-3	81.3	202.8	2.0	6.95	C30		70
SA-T600-100-4	88.9	170.0	2.0	4.71	C30		100

Note: The letter group "SA" in the specimen code represents steel-concrete beams, and the letter "T" indicates the heating temperature. K_0 refers to the initial stiffness value of the specimen, and the secant stiffness at P=0.4P_u is taken as the initial stiffness of the specimen. θ represents the shear span ratio, where θ=a/h0, a stands for the length of the shear span, and h_0 is the effective height of the cross-section. f_u denotes the peak load, and λ represents the replacement rate of recycled aggregates.

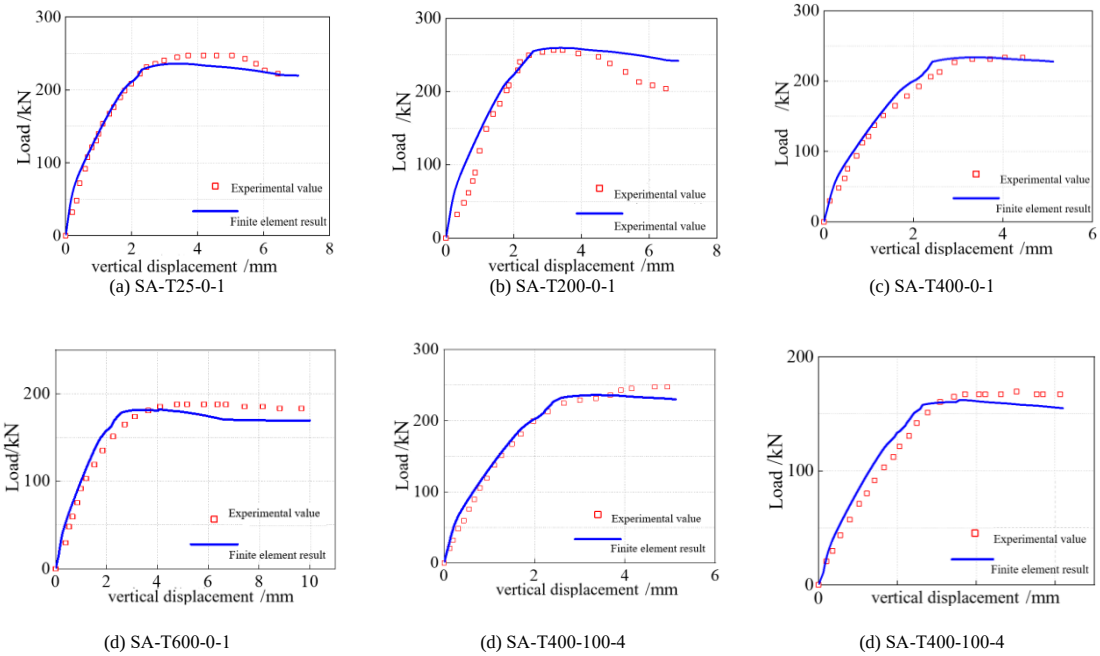

(a) SA-T25-0-1 (b) SA-T200-0-1 (c) SA-T400-0-1

(d) SA-T600-0-1 (d) SA-T400-100-4 (d) SA-T400-100-4

Fig. 6 Comparison of section steel recycled concrete beam test and finite element results

(a) Temperature distribution at mid-span at 400° C (b) Temperature distribution at mid-span at 600° C

Fig. 7 Temperature field distribution of section steel recycled concrete beams

The temperature distribution of the heated specimen is shown in Fig. 7, as can be seen, the surface temperature of the steel-concrete beam is higher when being heated. Due to the low thermal conductivity of concrete, outside-in heat transfer is relatively slow, exhibiting a significant thermal inertia. Conversely, steel experiences faster heat transfer.

The simulated results of the specimens are shown in Fig. 8. It can be observed from Fig. 7(a) to Fig. 7(b) that the steel-reinforced recycled concrete beams undergo deformation within the plane only without out-of-plane torsional deformation. The analysis based on Fig. 8(c) indicates that the failure mode of the steel-ECC composite beam simulated by using finite element method is flexural failure. Fig. 8(b) shows that the tensile damage simulated by using the finite element method reproduces the cracking pattern of the steel-reinforced recycled concrete beams. Fig. 8(d) illustrates the stress and deformation of the steel beams and steel reinforcement cages in the finite element model. It can be concluded that the finite element model can be used to accurately analyze the failure mode of steel-reinforced recycled concrete beams.

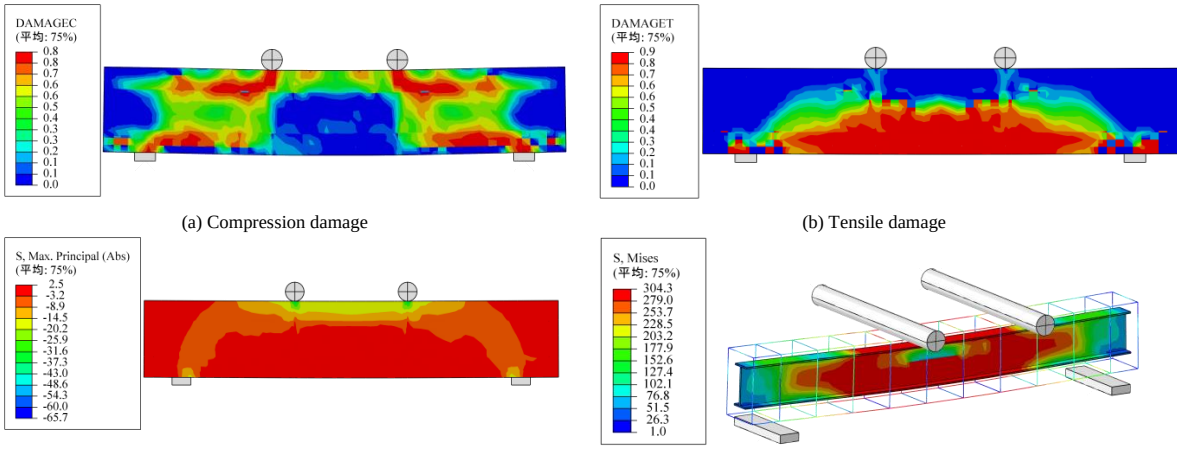

(a) Compression damage (b) Tensile damage

(c) Principal tensile stress (d) Stress and deformation of steel beam and steel reinforcement cage

Fig. 8 Simulation results of section steel recycled concrete beam

3. Parameter analysis

3.1. GFRP reinforcement for tension members

The type I strengthening method involves using GFRP tendons to reinforce the steel-reinforced recycled concrete beams, with the reinforcement configuration shown in Fig. 9. The strength of GFRP tendons under normal temperature and high temperature is shown in Table 2 [40]. Fig. 10(a) shows the analysis of the load-displacement curves of steel-reinforced recycled concrete beams with different diameters (4mm, 6mm and 8mm) under a fire temperature of 600°C, and a replacement ratio of 100%. As can be seen from the diagram, the curves based on different GFRP tendon diameters are similar at the elastic

stage. The ultimate load-carrying capacity of the members increases with the increase of GFRP tendon diameter. Compared to the unreinforced specimens, the ultimate load-carrying capacity of the 4mm, 6mm and 8mm GFRP tendon-steel-reinforced recycled concrete beam was increased by 6.38%, 13.03% and 22.35%, respectively. Fig. 10(b) illustrates the analysis of the load-displacement curves of steel-reinforced recycled concrete beams with different spacing (50mm, 75mm and 100mm) of GFRP tendons under a fire temperature of 600°C and a replacement ratio of 100%. By changing the spacing of the tendons, as can be seen, compared to the unreinforced specimens, the ultimate load-carrying capacity of the GFRP tendon-steel-reinforced recycled concrete beams was increased by 4.79% at a spacing of 100mm, 12.80% at a spacing of 75mm, and 16.74% at a spacing of 50mm, respectively.

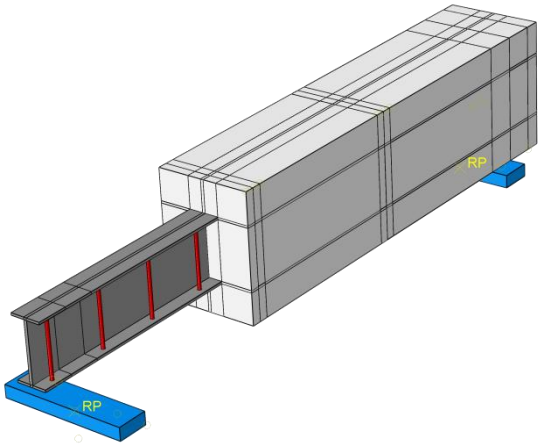

Fig. 9 Type I reinforcement method

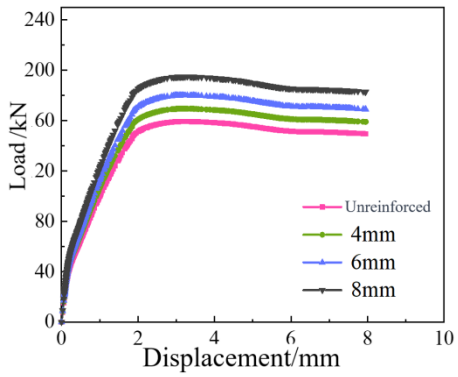

(a) Diameter of GFRP reinforcement bar

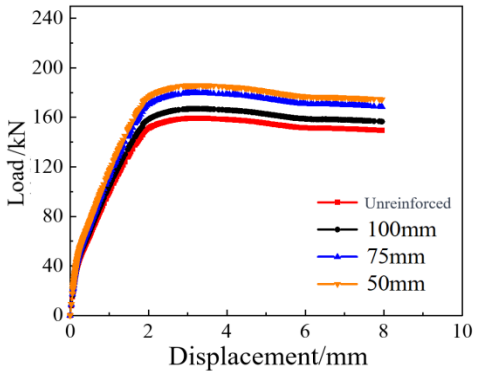

(b) Spacing between GFRP reinforcement bars

Fig. 10 Parametric analysis of Type I reinforcement method

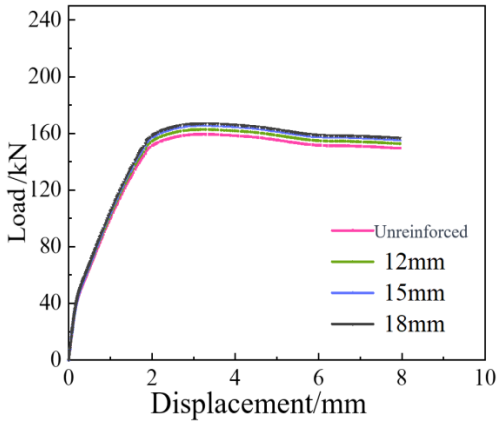

Fig. 11 Parametric analysis of Type II reinforcement method-longitudinal rib diameter

3.3. GFRP strength

Table 2
Mechanical properties of GFRP ribs at room temperature and high temperature

Heating temperature/°C	Elastic modulus/GPa	Tensile strength/MPa
20	32.8	884.6
50	28.7	774.0
100	24.6	663.5
150	20.5	552.9
200	16.4	442.3
250	12.3	331.7
300	8.2	221.2
350	4.1	110.6

3.2. Longitudinal reinforcement with GFRP bars

Type II strengthening method involves the use of GFRP longitudinal bars to reinforce the steel-reinforced recycled concrete beams. Fig. 11 shows the analysis of the load-displacement curves of steel-reinforced concrete beams in different diameters (12mm, 15mm and 18mm) of GFRP bars under a fire temperature of 600°C and a substitution rate of 100%. As can be seen, in the elastic stage, the curves based on different diameters of GFRP bars are essentially the same. For the ultimate load of each component, the increase of the diameter of GFRP longitudinal bars can increase the ultimate bearing capacity of the component. Compared to the ordinary specimens, the ultimate bearing capacity of the steel-reinforced concrete beams was increased by 2.14% with 12mm GFRP bars, 3.89% with 15mm GFRP bars, and 4.67% with 18mm GFRP bars.

Parameter analysis of the ultimate bearing capacity of steel-concrete beams with different reinforcement material strengths is conducted for Type I and Type II strengthening methods. The tensile strength of the reinforcement material is set as the original strength including 1000MPa, 1100MPa and 1200MPa. Fig. 12(a) presents the load-displacement curves of steel-concrete beams with different strengths of GFRP reinforcement (diameter of 4mm) using Type I strengthening method under a fire temperature of 600°C and a replacement ratio of 100%. In the elastic stage, the curves are generally consistent for different GFRP reinforcement strengths, and with the increase of GFRP reinforcement strength, the ultimate bearing capacity of the components increases. Compared to the specimens with original strength, the ultimate bearing capacity of GFRP-reinforced steel-concrete beams is increased by 1.97% with 1000MPa, 3.86% with 1100MPa, and 5.97% with 1200MPa. Fig. 12(b) shows the load-displacement curves of steel-concrete beams with different strengths of GFRP reinforcement (with the diameter of 4mm) using the Type II strengthening method at a fire temperature of 600°C and a replacement ratio of 100%. At the elastic phase, the curves based on different GFRP reinforcement strengths are generally consistent, and with the increase of GFRP reinforcement strength, the ultimate bearing capacity of the components increases. Compared to the specimens with original strength, the ultimate bearing capacity of GFRP-reinforced steel-concrete beams was increased by 1.15% with 1000MPa, 2.04% with 1100MPa, and 3.37% with 1200MPa.

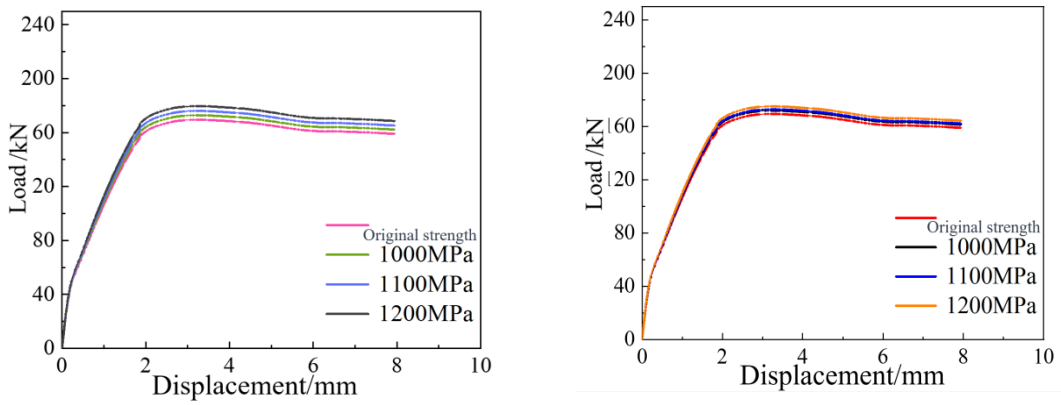

(a) Reinforcement method Type I (b) Reinforcement method Type II

Fig. 12 Analysis of reinforcement strength parameters

4. Conclusion

In this study, the influence of reinforcement methods and reinforcement material strength on the ultimate load-carrying capacity of GFRP-steel reinforced concrete beams was explored, and the load-carrying mode and failure mechanism of GFRP-steel reinforced concrete beams were analyzed. The following conclusions are drawn as follows:

(1) In a high-temperature fire environment, there is a noticeable temperature lag between the interior steel and GFRP reinforcement surfaces compared to the surface of the steel-concrete composite beams.

(2) A refined GFRP-SARC beam model was established by incorporating nonlinear material mechanics and bond-slip models for steel-reinforced concrete beams. The finite element model constructed by using ABAQUS software can predict the flexural performance of GFRP-steel-reinforced concrete beams accurately and effectively. Full-scale tests on six composite beam specimens revealed that the bending load-carrying capacity predicted by the finite element analysis deviated by an average of approximately 2% from the experimental results, while the flexural stiffness deviated by an average of approximately 3%.

(3) The Type I strengthening method significantly improves the load-carrying capacity of steel-reinforced recycled concrete beams. The load-carrying capacity of the tested beams is greatly affected by temperature, which is decreased by approximately 13% after exposure to a temperature of 200°C, and around 25% after exposure to a temperature of 600°C without strengthening. After being treated at the temperature of 600°C, the Type I strengthening method exhibited an average increase in load-carrying capacity of 10% compared to the unreinforced specimens, while the Type II strengthening method showed an average increase of approximately 4.7%.

(4) The Type I strengthening method is a key influencing parameter for the flexural behavior of steel-reinforced recycled concrete beams. The proposed Type I strengthening method can significantly enhance the load-carrying capacity of SARC beams, while providing higher safety reserves.

Acknowledgment

The authors thank Dr. Qi Guo, a professor at Xi'an University of Science and Technology in Xi'an, Shaanxi Province, China, for helping explain the significance of the findings of this study.

References

[1] Ghalehnovi M, Roshan N, Hakak E, et al. Effect of red mud (bauxite residue) as cement replacement on the properties of self-compacting concrete incorporating various fillers[J]. Journal of Cleaner Production, 2019, 240: 118213.
[2] Meghdadian M, Gharaei-Moghaddam N, Arab Shahi A, et al. Proposition of an equivalent reduced thickness for composite steel plate shear walls containing an opening[J]. Journal of Constructional Steel Research, 2020, 168: 105985.
[3] Huang Jingyi, Zhu Dayong, Gao Peng, Zhou An, Dai Liangjun. Research on seismic performance of BFRP reinforced high axial compression ratio and low strength concrete columns [J]. Journal of Building Materials, 2020,23 (06): 1366-1373
[4] Huang Jingyi. Research on Seismic Performance of Low Strength Concrete Reinforced Columns Strengthened with Basalt Fiber Composite Materials [D]. Hefei University of Technology, 2020.
[5] Lian Yu, Xiao Ru-cheng, Sun Bin, Cheng Jin, Jia Lijun, Zhuang Dong-li. Static characteristics of GFRP composite bridge decks reinforced with rivets and self-tapping screws [J]. China Journal of Highway and Transport, 2016,29 (10): 54-65,94.
[6] Etxeberria M, Vázquez E, Marí A, et al. Influence of amount of recycled coarse aggregates and production process on properties of recycled aggregate concrete[J]. Cement and concrete research, 2007, 37(5): 735-742.
[7] Yehia S, Helal K, Abusharkh A, et al. Strength and durability evaluation of recycled aggregate concrete[J]. International journal of concrete structures and materials, 2015, 9(2): 219-239.
[8] McNeil K, Kang H K. Recycled Concrete Aggregates: A Review, International Journal of Concrete Structures and Materials[J]. 2013.
[9] Xie T, Gholampour A, Ozbakkaloglu T. Toward the development of sustainable concretes with recycled concrete aggregates: comprehensive review of studies on mechanical properties[J]. Journal of Materials in Civil Engineering, 2018, 30(9): 04018211.
[10] Ozbakkaloglu T, Gholampour A, Xie T. Mechanical and durability properties of recycled aggregate concrete: effect of recycled aggregate properties and content[J]. Journal of Materials in Civil Engineering, 2018, 30(2): 04017275.
[11] Liu Yibin, Cao Wanlin, Xing Feng, et al. Full-scale test of flexural performance of steel reinforced recycled concrete beams [J]. Building Structure, 2023,53 (09): 108-114.
[12] Wang Bing, You Hong Xu, Liu Xiao. Research on the bending behavior of recycled steel reinforced concrete beams after high temperature [J]. Engineering Mechanics, 2018, 35 (S1): 161-165,180.
[13] Li Yuanyuan. Experimental and Numerical Simulation Study on the Bending Performance of Steel Reinforced Recycled Concrete Beams [D]. Hebei University of Engineering, 2015.
[14] Ke X, Tang Z, Yang C. Shear bearing capacity of steel-reinforced recycled aggregate concrete short beams based on modified compression field theory[C]//Structures. Elsevier, 2022, 45: 645-658.
[15] Chen Z P, Chen Y L, Zhong M. Shear performance test and bearing capacity calculation of steel reinforced recycled coarse aggregate concrete beam[J]. Journal of Experimental Mechanics, 2014, 29(1): 97-104.
[16] Jian yang X, Xiu Zhen W, Hui M. Experimental study on shear performance of steel reinforced recycled aggregate concrete beams[J]. Building Structure, 2013, 43(7): 69-72.
[17] Al Mahmoud F, Boissiere R, Mercier C, et al. Shear behavior of reinforced concrete beams made from recycled coarse and fine aggregates[C]//Structures. Elsevier, 2020, 25: 660-669.
[18] Arezoum andi M, Steele A R, Volz J S. Evaluation of the bond strengths between concrete and reinforcement as a function of recycled concrete aggregate replacement level[C]//Structures. Elsevier, 2018, 16: 73-81.
[19] Thomas J, Thaickavil N N, Wilson P M. Strength and durability of concrete containing recycled concrete aggregates[J]. Journal of Building Engineering, 2018, 19: 349-365.
[20] Pliya P, Hajiloo H, Romagnosi S, et al. The compressive behavior of natural and recycled aggregate concrete during and after exposure to elevated temperatures[J]. Journal of Building Engineering, 2021, 38: 102214.
[21] Gao D, Zhu W, Fang D, et al. Shear behavior analysis and capacity prediction for the steel fiber reinforced concrete beam with recycled fine aggregate and recycled coarse aggregate[C]//Structures. Elsevier, 2022, 37: 44-55.
[22] Anike E E, Saidani M, Olubanwo A O, et al. Flexural performance of reinforced concrete beams with recycled aggregates and steel fibres[C]//Structures. Elsevier, 2022, 39: 1264-1278.
[23] Pour A K, Shirkhani A, Zeng J J, et al. Experimental investigation of GFRP-RC beams with Polypropylene fibers and waste granite recycled aggregate[C]//Structures. Elsevier, 2023, 50: 1021-1034.
[24] Tariq F, Ahmad S. Mechanical and bond properties of completely recycled aggregate in concrete exposed to elevated temperatures[C]//Structures. Elsevier, 2023, 56: 104979.
[25] Chen Z, Liao H, Zhou J, et al. Eccentric compression behavior of reinforced recycled aggregate concrete columns after exposure to elevated temperatures: Experimental and numerical study[C]//Structures. Elsevier, 2022, 43: 959-976.
[26] Xue Jian yang, Wang Xiuzhen, Ma Hui, Lin Jianpeng, Chen Zongping. Experimental study on shear performance of steel reinforced recycled concrete beams [J]. Building Structure, 2013,43 (07): 69-72
[27] Wu Ping Chuan, Xie Lulu, Li Yuanyuan, Zhao Shuli. Experimental study on the flexural performance of steel reinforced recycled concrete beams [J]. Journal of Hebei Engineering University (Natural Science Edition), 2016,33 (01): 31-34
[28] Chen Zongping, Zheng Huahai, Xue Jian yang, Su Yi sheng. Bond slip test and bond strength analysis of steel reinforced recycled concrete [J]. Journal of Building Structures, 2013,34 (05): 130-138. DOI: 10.14006/j.jzjgxb.2013.05.05.015
[29] Han Fei, Kong Xiangqing, Bao Chengcheng, Liu Huaxin, Zhang Wenjiao. Experimental study on the flexural performance of recycled concrete beams with BFRP reinforcement [J]. Fiberglass reinforced plastic/composite materials, 2017 (12): 45-50
[30] Chen Zhongping, Zheng Wei, Xue Jian yang, et al. Bending test and bearing capacity calculation of steel reinforced recycled concrete beams after high temperature [J]. Industrial Architecture, 2014,44 (11): 45-50.
[31] Lu Chunhua, Ping An, Yan Yong Dong, Zhang Julian. Experimental study on tensile properties and Strength reduction calculation of GFRP/BFRP bars after high temperature action [J/OL]. Journal of Harbin Engineering University: 1-8.
[32] Gao Yong Hong, Tian Yun, Jin Qingping. Study on the effect of temperature on the tensile mechanical properties of GFRP reinforcement [J]. Plastic Industry, 2016,44 (09): 95-99。
[33] GB50017-2017. Code for Design of Steel Structures [S]. China Planning Press

[34] WANG Q H, YANG J S, LIANG Y Z, et al. Prediction of time-dependent behavior of steel-recycled aggregate concrete(RAC)composite slabs via thermo-mechanical finite element modeling[J]. Journal of Building Engineering, 2020, 29: 101191.
[35] CEN. Eurocode 2: design of concrete structure-part 1-1: general rules and rules for buildings: ENV 1992-1-2 [S]. Brussels: Europe Committee for Standardization(CEN), 2004.
[36] DE JUAN M S, GUTIÉRREZ P A. Study on the influence of attached mortar content on the properties of recycled concrete aggregate[J]. Construction and Buildings Materials, 2009, 23(2):872-877.
[37] XIAO J Z, LI W G, FAN Y H, et al. An overview of study on recycled aggregate concrete in China(1996-2011)[J]. Construction and Building Materials, 2012,(31): 364-383.
[38] LIU Q, XIAO J Z, SUN Z H. Experimental study on the failure mechanism of recycled concrete[J]. Cement and Concrete Research, 2011, 41(10): 1050-1057.
[39] Chen Z P, et al. Mechanical behavior and bearing capacity calculation of steel reinforced recycled concrete beam after experiencing high temperature [J]. China Civil Engineering Journal.2016, 49(2): 49—58.
[40] Chunhua LU, Zhong Hao QI, Hao GE, et al. Experimental and theoretical investigation on shear performance degradation of GFRP bars in concrete after fire and high temperature[J]. Acta Materiae Compositae Sinica.